

**SPECIAL FOCUS: ANIMAL MODELS IN TISSUE ENGINEERING. PART I\***

## Age-Dependent Subchondral Bone Remodeling and Cartilage Repair in a Minipig Defect Model

Christian G. Pfeifer, MD,<sup>1-3</sup> Matthew B. Fisher, PhD,<sup>1,2,\*\*</sup> Vishal Saxena, MD,<sup>1,2</sup> Minwook Kim, PhD,<sup>1,2,4</sup> Elizabeth A. Henning, MS,<sup>1,2,4</sup> David A. Steinberg, MD,<sup>1,2</sup> George R. Dodge, PhD,<sup>1,2,5</sup> and Robert L. Mauck, PhD<sup>1,2,4,5</sup>

After cartilage injury and repair, the subchondral bone plate remodels. Skeletal maturity likely impacts both bone remodeling and inherent cartilage repair capacity. The objective of this study was to evaluate subchondral bone remodeling as a function of injury type, repair scenario, and skeletal maturity in a Yucatan minipig model. Cartilage defects (4 mm) were created bilaterally in the trochlear groove. Treatment conditions included a full thickness chondral defect (full chondral defect,  $n = 3$  adult/3 juvenile), a partial thickness ( $\sim 50\%$ ) chondral defect (PCD,  $n = 3/3$ ), and FCD treated with microfracture (MFX,  $n = 3/3$ ). At 6 weeks postoperatively, osteochondral samples containing the lesion site were imaged by micro-computed tomography (CT) and analyzed by histology and immunohistochemistry. Via micro-CT, FCD and MFX groups showed increased bone loss in juveniles compared with adults. Quantification of histology using the ICRS II scoring system showed equal overall assessment for the FCD groups and better overall assessment in juvenile animals treated with MFX compared with adults. All FCD and MFX groups were inferior to control samples. For the PCD injury, both age groups had values close to the control values. For the FCD groups, there were greater alterations in the subchondral bone in juveniles compared with adults. Staining for collagen II showed more intense signals in juvenile FCD and MFX groups compared with adults. This large animal study of cartilage repair shows the significant impact of skeletal maturity on the propensity of subchondral bone to remodel as a result of chondral injury. This will improve selection criteria for animal models for studying cartilage injury, repair, and treatment.

**Keywords:** subchondral bone, cartilage, microfracture, skeletal maturity

### Introduction

**G**IVEN THE HIGH PREVALENCE of focal cartilage injuries and the propensity for such defects to instigate the early onset of osteoarthritis, a number of surgical treatment options to enhance cartilage repair have been developed. Techniques involving the subchondral bone, for example, microfracture (MFX), as well as techniques that do not disturb the cement line, for example, autologous chondrocyte implantation (ACI), are commonly employed. Although such treatments can positively impact regeneration of cartilage, they may have unwanted effects on the underlying bone. For example, after treatment by MFX or ACI, subchondral bony remodeling has been reported, ranging in severity from upward bony migration<sup>1-4</sup> to the formation of intralesional osteophytes or cysts.<sup>5-7</sup> This phenomenon is

also known to cause clinical complications, such as failure of graft integration, enlargement of the initial defect, and subchondral edema, which may lead to overall treatment failure rather than to repair of the impaired cartilage.

In keeping with these clinical observations, basic science studies using large animal models, including canine,<sup>8</sup> caprine,<sup>9</sup> and porcine,<sup>10</sup> also show changes in subchondral bone during repair of full thickness chondral defects. Likewise, in both small and large animal studies involving MFX, upward subchondral bone plate migration is commonly reported.<sup>11-13</sup> Thus, the osteochondral unit must be restored to ensure a meaningful cartilage repair,<sup>14</sup> and care should be taken to verify that the animal model employed accurately reflects the changes that occur in humans.

One aspect to this bone remodeling response after cartilage repair may be the age of the subject. Bone remodeling

<sup>1</sup>Department of Orthopaedic Surgery, University of Pennsylvania, Philadelphia, Pennsylvania.

<sup>2</sup>Translational Musculoskeletal Research Center, Philadelphia VA Medical Center, Philadelphia, Pennsylvania.

<sup>3</sup>Department of Trauma Surgery, Regensburg University Medical Center, Regensburg, Germany.

<sup>4</sup>Department of Bioengineering, University of Pennsylvania, Philadelphia, Pennsylvania.

<sup>5</sup>Collaborative Research Partner (CRP), Acute Cartilage Injury (ACI) Program of the AO Foundation, Davos, Switzerland.

\*\*Current affiliation: Department of Biomedical Engineering, University of North Carolina – Chapel Hill, Chapel Hill, North Carolina and North Carolina State University, Raleigh, North Carolina.

\*This article is part of a special focus issue on Animal Models in Tissue Engineering. Part I.

occurs throughout life, and age-dependent differences exist due to normal growth and maturation as well as due to metabolic bone diseases, such as osteoporosis. Although remodeling slows with age,<sup>15,16</sup> limited information exists in terms of whether subchondral remodeling after cartilage damage is also age dependent. Given the importance of the osteochondral unit for functional repair of the articular surface, age-related limitations of cartilage repair might be associated with age-related changes in subchondral bone remodeling.

Because subchondral bone remodeling could compromise outcomes of tissue-engineered cartilage repair, the objective of this study was to evaluate subchondral bone remodeling as a function of injury type, repair scenario, and age in a Yucatan minipig model of cartilage injury. To address this issue, we investigated the response of the subchondral bone to full chondral defects with removal of the calcified cartilage layer as well as partial chondral defects that maintained the integrity of the calcified cartilage layer. Further, since skeletal maturity likely impacts both bone remodeling (due to changes in subchondral bone activity) and inherent cartilage repair capacity (due to changes in endogenous stem cell populations and reduced cell number), both skeletally mature and immature groups were evaluated.

## Materials and Methods

### *Animal model and surgical procedure*

To carry out this study, surgery was performed on the stifle joints of three juvenile (6 months, male, 32.9–37.7 kg) and three skeletally mature (18 months of age, male, 62.0–64.0 kg) Yucatan minipigs (Sinclair Bioresources) with IACUC approval from the Philadelphia VA Medical Center and the University of Pennsylvania. All animal procedures were performed in accordance with policies set forth by the National Institutes of Health.

Preoperative medication consisted of ketamine (11–33 mg/kg intramuscular [i.m.]), xylazine (2.2 mg/kg), and cephalexin (250 mg orally [p.o.]). After induction, maintenance of general anesthesia and pain control was achieved with isoflurane (1–4 vol.%, inh.), buprenorphine (0.01 mg/kg i.m.), and saline (10–20 mL/h, intravenously [i.v.]). To access the trochlear groove, a 7 cm (2.7 inches) long skin incision was made over the medial aspect of the patella. After a lateral arthrotomy, the patella was subluxed to the medial side to expose the trochlear groove. In each animal, four 4 mm diameter defects were created in the trochlear groove (three of these were used for the current study). Details on all four defects have been previously described (10). Treatment conditions for these defects included an untreated full thickness chondral defect (FCD,  $n=3$  adult/3 juvenile), where the cartilage including the calcified layer was removed; a partial thickness chondral defect (PCD,  $n=3/3$ ), where ~50% of the cartilage was removed; and a full thickness chondral defect that was treated with MFX ( $n=3/3$ ). Treatment localizations within the trochlear groove were randomized from joint to joint. After soft tissue and skin closure, the superficial incision sites were injected with a local anesthetic (Bupivacaine, 0.25% solution, 5 mL per incision).

After extubation and recovery, pigs were allowed full weightbearing as tolerated. Postoperative analgesia consisted of buprenorphine (0.01 mg/kg i.m., 2×/day) for the first 3 days postsurgery and carprofen (2–3 mg, 1×/day, p.o.)

for 5 days postsurgery. Cephalexin (250 mg/day p.o.) was administered until postoperative day 3.

Animals were euthanized after 6 weeks postoperatively after premedication with ketamine (11–33 mg/kg i.m.) and xylazine (2.2 mg/kg), followed by intravenous overdose of pentobarbital (80 mg/kg) and phenytoin sodium (10 mg/kg). The stifle joints were harvested, and skeletal immaturity or maturity was confirmed by fluoroscopy.

### *Gross view imaging and scoring*

Digitized gross view images of the trochlear groove were taken after soft tissue dissection. All images were saved, randomized, and blinded for macroscopic scoring. Four blinded reviewers scored all 18 treated defects according to a semi-quantitative, 5-item scoring system (color, presence of blood vessels, surface of the repair tissue, adjacent cartilage, and defect fill), described by Goebel *et al.*,<sup>17</sup> wherein higher scores indicate inferior macroscopic appearance. Scores were averaged across the reviewers.

### *Micro-computed tomography analysis*

Osteochondral plugs inclusive of one defect area were then separated from the trochlear groove by use of a hand saw and fixed in 4% paraformaldehyde (Affymetrix, Santa Clara, CA). One adjacent osteochondral plug per joint served as control. Micro-computed tomography (CT) scans for all specimens were performed by using a VivaCT 75 (Scanco, Wayne, PA). Specimens were scanned at 55 kVp and 145 A to image the bone. After this primary scan, samples were immersed in Lugol's solution (Sigma, St. Louis, MO) for 48 h and subjected to a second scan to visualize the cartilage and allow for calculation of the defect fill. For further analysis, depth-dependent cylindrical volumes of interest (VOI) were calculated in each sample as previously described.<sup>10</sup> Within each VOI, the bone volume per total volume (BV/TV), trabecular spacing, trabecular number, and trabecular thickness was computed and its relative value compared with the specific range of the control from the same joint was calculated. Additional full three-dimensional (3D) reconstructions of each specimen were generated for visualization purposes.

### *Histology*

After micro-CT, specimens were decalcified (Formical-2000; Thermo Fisher Scientific, Pittsburgh, PA) for 10 days, embedded in paraffin, and sectioned at a thickness of 6  $\mu$ m. For each sample, hematoxylin and eosin (H&E) and Safranin-O/fast green (Saf-O) staining was performed according to standard protocols. Sections were microscopically analyzed for cell and defect morphology (H&E) and matrix content (fibrous tissue and proteoglycans, Saf-O). Three blinded reviewers scored the histological images according to the ICRS II semi-quantitative scoring scale.<sup>18</sup> Scores were averaged among reviewers, and statistical analysis was carried out as described later.

### *Immunohistochemistry and evaluation of defect fill by digital image analysis*

Immunohistochemistry for collagen type II was performed to evaluate cartilage regeneration and collagen II matrix distribution. To do so, paraffin sections were deparaffinized,

rehydrated, and subjected to proteinase K antigen retrieval for 15 min at 37°C. Sections were incubated with a type II collagen antibody (5 µg/mL; Developmental Studies Hybridoma Bank, University of Iowa, Iowa City, IA) for 1 h. After washing, the signal was detected by using the Millipore Immunoperoxidase Secondary Detection System (EMD Millipore Corporation, Billerica, MA). After digital imaging, defects were analyzed for proportional collagen type II stain within the defect fill.

For all stains, images were acquired under bright-field illumination by using a Nikon Eclipse NI-E (Nikon, Tokyo, Japan). Images were acquired at a magnification of 10× and stitched by using the NIS-Elements AR 4.2 (Nikon) software. For quantification of collagen type II stain, images were converted to grayscale, and the area of the defect fill was outlined exclusive of the remodeling subchondral bone. After thresholding, the amount of positive staining was computed as the number of black (positive) pixels was divided by the total number of pixels within the outlined defect fill and multiplied by 100 and given as percentage (ImageJ; National Institutes of Health, Bethesda, MD).

#### Statistical analysis

Statistical analysis was carried out by using SPSS® (version 20; IBM, Armonk, NY). The Kolmogorov-Smirnov test was used to check for normal distribution. For BV/TV, macroscopic scoring, and collagen type II scoring, all values were normally distributed. A two-way analysis of variance (ANOVA) with group and age as independent factors followed with individually performed posthoc tests to maintain an overall alpha level at  $p < 0.05$ . Similar procedures were

used for ICRS II scores, where some datasets were normally distributed and others not. For non-normal distributions, a Kruskal-Wallis test followed by an individual Mann-Whitney test was used. To control for type-1 error, a Bonferroni correction for multiple comparisons ( $p < 0.006$ ) was applied.

## Results

### Animal surgeries

All surgeries were performed without intra- or postoperative complications. During surgery, a marked difference in cartilage thickness between adult and juvenile minipigs was observed, with juvenile minipigs having thicker cartilage at all locations throughout the trochlear groove relative to adult animals. Cartilage removal in adult minipigs was more laborious, as the cartilage was better integrated with the calcified layer. All pigs were weightbearing on all fours at postoperative day 1, and no signs of infection were observed during the follow-up period or after dissection at time of euthanasia.

### Fluoroscopy and macroscopic evaluation

Posteuthanasia, defects of the adjacent cartilage were clearly visible in adult minipigs in the FCD, MFX, and PCD groups abnormalities in adjacent cartilage marked with asterisk (\*). These defects were not seen in juvenile specimens despite similar surgical techniques. Fluoroscopic imaging showed fused femoral and tibial growth plates in the adult minipigs (Fig. 1b), whereas skeletally immature pigs had open physes in both the femur and tibia (Fig. 1c). Although no significant differences were observed, data

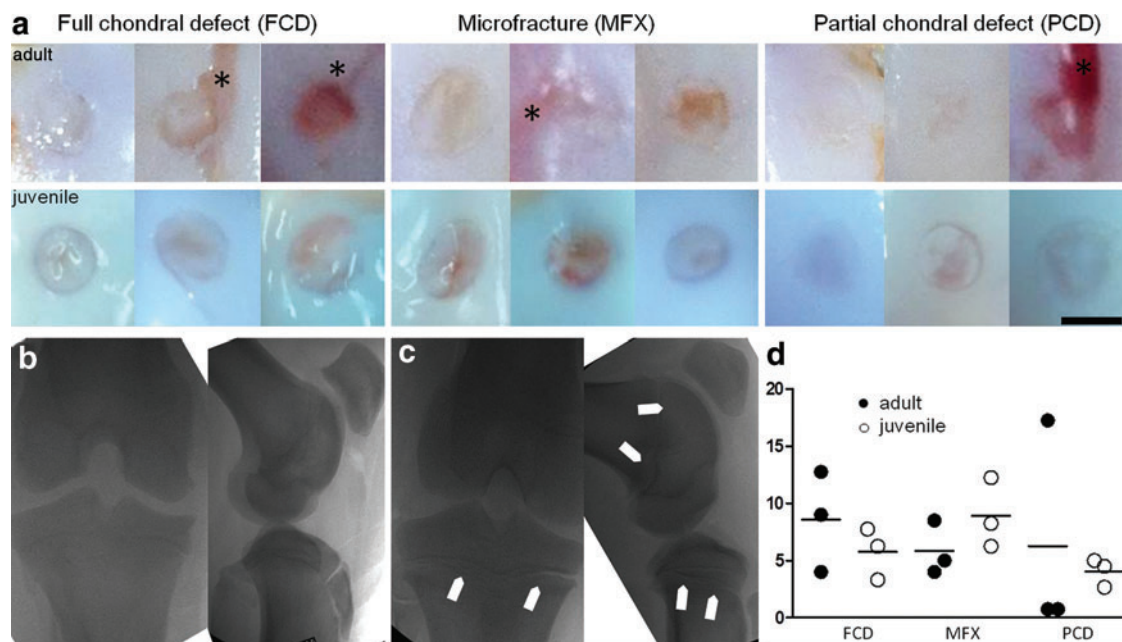


**FIG. 1.** (a) Macroscopic images of lesions at 6 weeks postoperatively; lesions of adjacent cartilage are visible in adult minipig specimens (\*); scale bar = 4 mm. (b) Fluoroscopic image of an adult minipig stifle joint in tunnel and sagittal view; tibial and femoral growth plates are closed. (c) Fluoroscopic image of juvenile minipig stifle joint in tunnel and sagittal view; tibial and femoral physes are open, as indicated by arrow heads. (d) Macroscopic scoring at 6 weeks postoperatively according to Goebel *et al.*, where higher scores represent a worse appearance (worst score = 20 points, best score = 0 points); full circles = adult minipigs; empty circles = juvenile minipigs. Color images available online at [www.liebertpub.com/tec](http://www.liebertpub.com/tec)

from macroscopic scoring showed that the mean values for full chondral defects (6.1 [SD 2.3]) and partial chondral defects (4.3 [SD 1.8]) were lower in skeletally immature minipigs compared with skeletally mature minipigs. Conversely, in the MFX group, the mean value of mature minipigs was lower (5.8 [SD 2.6] vs. 8.9 [SD 3.7]) (Fig. 1d).

#### Micro-CT analysis

Micro-CT analysis revealed marked differences between adult and juvenile minipigs in terms of initial bony morphology and bony remodeling in the subchondral bone beneath cartilage lesion (Fig. 2). In control and defect specimens, absolute values for BV/TV were higher in adult minipigs compared with juvenile minipigs, regardless of defect type and depth of the analyzed subchondral bone. Values for BV/TV of control defects in adult animals were 69.2 in range 1, 52.4 in range 2, 48.1 in range 3, and 44.9 in range 4, respectively; whereas values in juvenile animals were 40.1 in range 1, 34.9 in range 2, 34.0 in range 3, and 31.6 in range 4. Qualitative analysis of bone beneath the cartilage defects showed, through 3D reconstructions, that FCD and MFX groups resulted in greater bone loss in skeletally immature minipigs compared with skeletally mature minipigs (Fig. 2). In the PCD group, there was a slight elevation of the subchondral plate in immature minipigs at 6 weeks postoperatively compared with mature minipigs (Fig. 2, lower left panel), which showed little change in subchondral architecture. Quantifying these observations in terms of BV/TV near the cartilage-bone interface (range 1), the FCD group for juvenile animals showed significantly lower values relative to adults ( $p < 0.05$ ), whereas the MFX and PCD groups were not significantly different between the juveniles and adults ( $p > 0.05$ , Fig. 3). Comparing between groups in the juvenile animals, the FCD group had significantly lower values relative to the PCD group ( $p < 0.05$ ). No significant differences were found between the groups in the adult animals ( $p > 0.05$ ) for range 1. With progression away from the

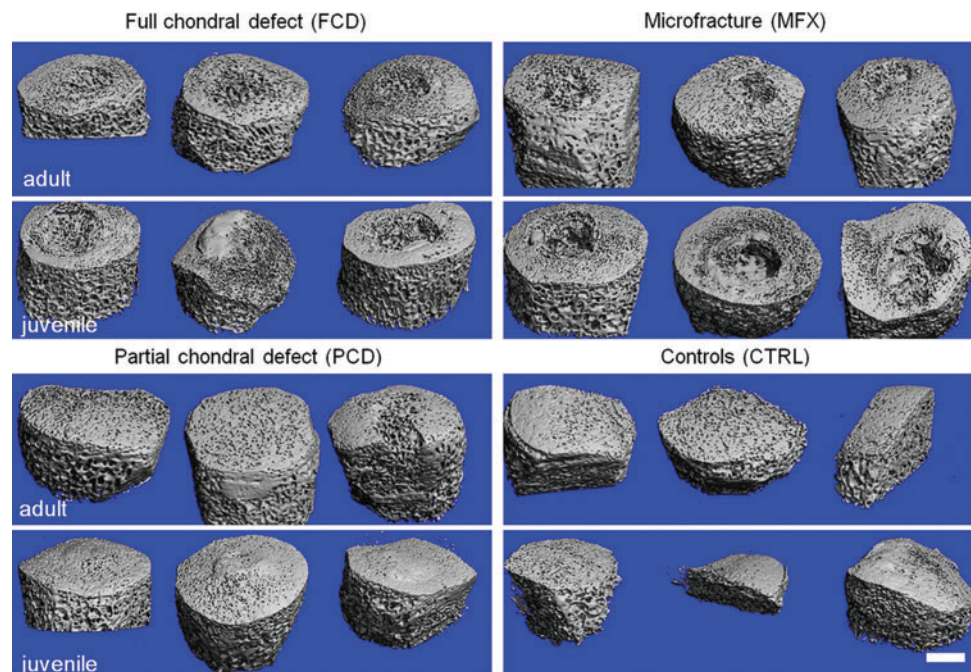
cartilage-bone interface, values for the skeletally immature pigs were not significantly different from values for the adult animals for ranges 2–4 ( $p > 0.05$ , Fig. 3). Qualitatively, all groups appear to reach similar relative values by range 4 with lower levels of variability. Statistical analyses revealed no significant effects due to age or experimental group for trabecular spacing, trabecular number, or trabecular thickness for any range ( $p > 0.05$ ) (Supplementary Figs. S1–S3; Supplementary Data are available online at [www.liebertpub.com/tec](http://www.liebertpub.com/tec)). Defect fill (Supplementary Fig. S4b) assessed from post-Lugols micro-CT was not significantly different between ages or treatment groups ( $p > 0.05$ ), but it tended to be higher in immature minipigs compared with mature minipigs.

#### Histology and immunohistochemistry

Histological analysis showed qualitatively better fill in juveniles, with some evidence of Safranin-O positive staining at 6 weeks postoperatively (Fig. 4). Defect fill in the adult and juvenile FCD groups mainly consisted of Safranin-O negative tissue, with no evidence of cartilage-specific extracellular matrix. In the juvenile MFX group, some Safranin-O positive tissue (indicative of proteoglycan deposition) was detected. All PCD groups showed a small layer of fibrous tissue on top of the remaining cartilage, and the remaining cartilage was stained nearly to the same extent as the adjacent noninjured cartilage (Fig. 5). In terms of subchondral remodeling, and consistent with the micro-CT analysis, mature minipigs showed less bone remodeling compared with immature minipigs.

Quantification of the histology using the ICRS II scoring system showed equal overall assessment for the FCD groups, better overall assessment for the juvenile MFX groups compared with adult MFX, and values close to the control samples for the PCD groups (Fig. 6). Overall assessment for juvenile minipigs was significantly lower for all treatment groups compared with age-related control groups ( $p < 0.05$ ).

**FIG. 2.** Micro-CT imaging of adult and juvenile subchondral bone after cartilage injury and repair. Juvenile minipigs showed significant bone loss 6 weeks postoperatively in both the FCD and MFX groups, whereas osseous overgrowth was visible in PCD. Adults showed little change in subchondral bone in any group other than MFX. Scale bar = 2 mm. CT, computed tomography; FCD, full chondral defects; MFX, microfracture; PCD, partial chondral defects. Color images available online at [www.liebertpub.com/tec](http://www.liebertpub.com/tec)



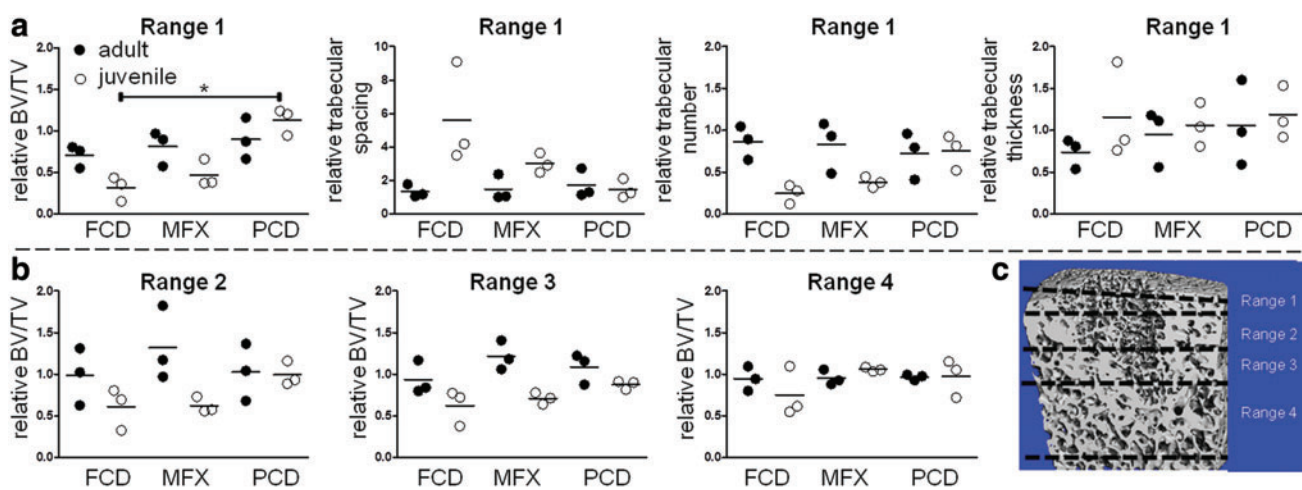


**FIG. 3.** (a) Micro-CT analysis of BV/TV, trabecular spacing, trabecular number, and trabecular thickness for the immediate underlying subchondral bone plate (range 1, see schematic). All values are provided as relative to control defects of adjacent, nontreated osteochondral samples. \* $p < 0.006$ . (b) Analysis of BV/TV as function of distance from the subchondral bone plate. The relative change in BV/TV approaches unity as depth increases, indicating similar BV/TV compared with controls in deeper zones. Significant differences ( $p < 0.05$ ) were detected for age in the overall two-way ANOVA in range 2 and range 3; *full circles*=adult minipigs; *empty circles*=juvenile minipigs. (c) Schematic of micro-CT analysis in each range (as a function of distance from the bone-cartilage interface). Scale bar = 1 mm. ANOVA, analysis of variance; BV/TV, bone volume per total volume. Color images available online at [www.liebertpub.com/tec](http://www.liebertpub.com/tec)

Further, for the FCD group, there was less alteration in the subchondral bone and a slightly better basal integration noted in mature compared with immature minipigs. Significantly different values for subchondral bone scores were found between adult and juvenile minipigs in the MFX groups, between the juvenile FCD and MFX groups, between the juvenile MFX and PCD groups, and between the juvenile MFX and the age-related control group ( $p < 0.05$ ). Likewise, the MFX group showed decreased basal integration in immature compared with mature minipigs (Fig. 6). However

statistical significance was not reached for basal integration between the juvenile FCD and PCD groups, between the juvenile FCD and age-related control groups, or between the juvenile MFX and age-related control groups ( $p > 0.05$ ). Additional scored parameters showed mainly lower values for FCD and MFX groups, regardless of age, compared with PCD or control conditions. Significant differences were found for clustering at middle/deep zone between juvenile FCD and PCD groups, as well as between juvenile FCD and age-related control groups and between juvenile MFX and age-

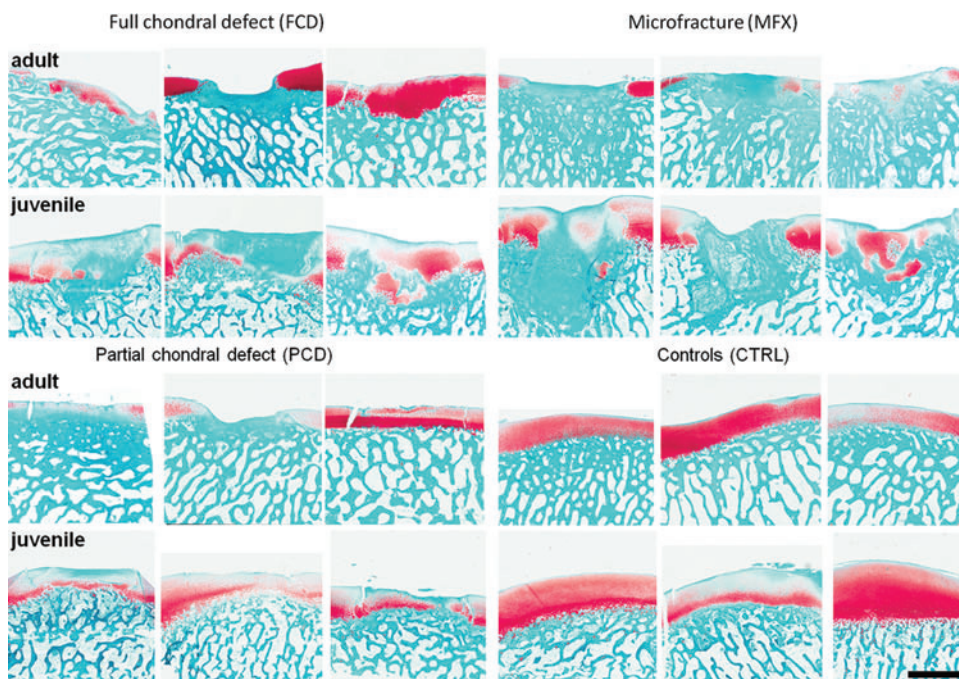


**FIG. 4.** Safranin-O/fast-green stain for proteoglycan visualization in cartilage repair tissue. All samples are shown from each defect group and age, depicting proteoglycan content of the repair cartilage. Scale bar = 2 mm. Color images available online at [www.liebertpub.com/tec](http://www.liebertpub.com/tec)

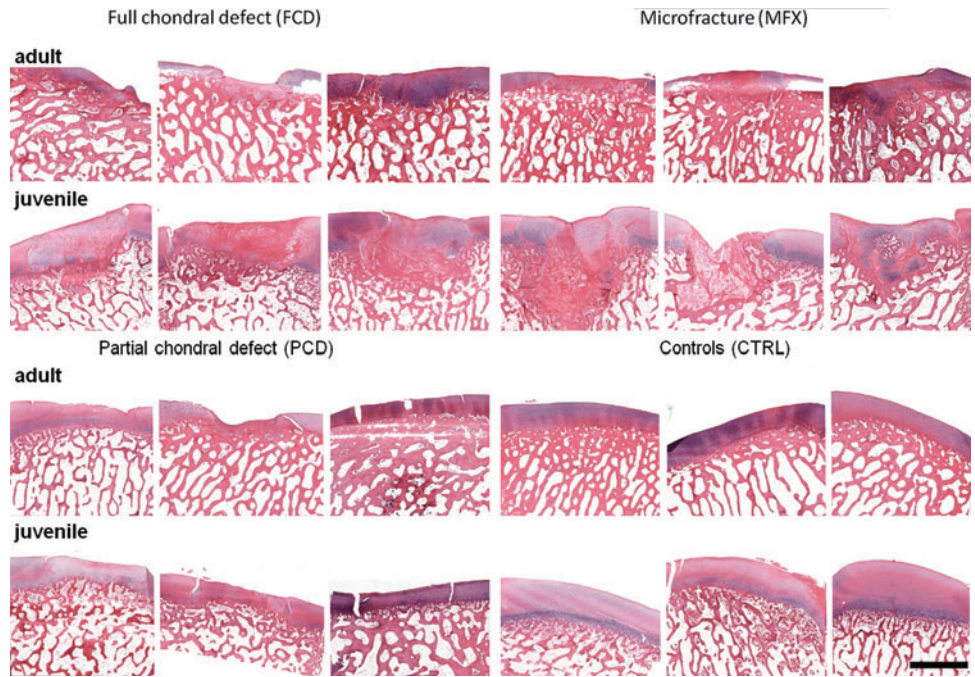


**FIG. 5.** H&E stain for visualization of cartilage repair tissue. All samples are shown from each defect group and age. Scale bar=2 mm. H&E, hematoxylin and eosin. Color images available online at [www.liebertpub.com/tec](http://www.liebertpub.com/tec)

related control groups ( $p < 0.05$ ). Scoring for surface architecture yielded statistically significant differences for the juvenile FCD group compared with the age-related control group ( $p < 0.05$ ). Differences in formation of a tidemark were statistically significant between juvenile FCD and PCD groups as well as between juvenile MFX and PCD groups; they were also statistically significant between juvenile FCD, juvenile MFX, and the age-related control group ( $p < 0.05$ ).

Immunohistochemical staining for collagen II showed a qualitative trend toward more intense signals in the repair tissue in immature FCD and MFX groups compared with the same repair groups in mature animals. Of interest in several samples (primarily juvenile samples), the remodeling

subchondral bone also stained for collagen II at this time point (Fig. 7). Digital image analysis (of the cartilage defect only) revealed that immature minipigs trended qualitatively toward higher collagen II in the repair tissue, regardless of treatment group, compared with mature minipigs (FCD: 55.3% collagen type II stain [SD 8.5] vs. 41.9% [SD 24.6]; MFX: 48.8% [SD 32.7] vs. 40.0% [SD 14.9]; PCD: 86.7% [SD 13.5] vs. 69.9% [SD 45], Supplementary Fig. S5).

**Discussion**

As subchondral bone remodeling has a large impact on the effectiveness of cartilage repair in clinics,<sup>14,19</sup> as well as

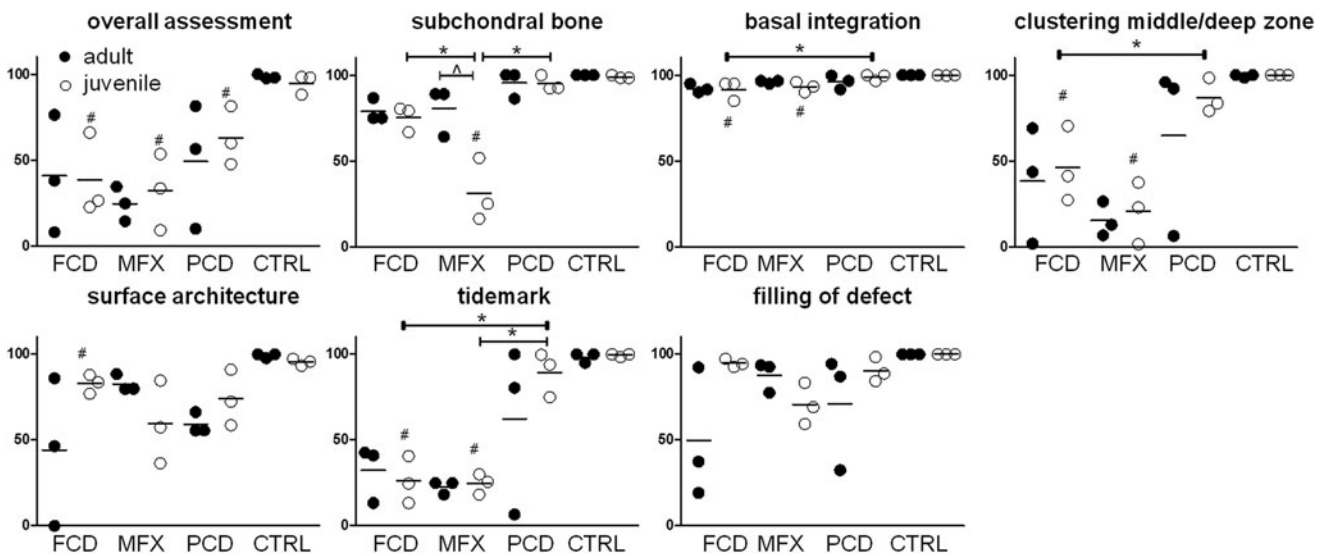


**FIG. 6.** ICRS II scoring of cartilage defects (additional categories are shown in Supplementary Fig. S4a), # $p < 0.006$  compared with age-adjusted control group; \* $p < 0.006$  between age-related groups; ^ $p < 0.025$  between ages within same treatment group. Full circles=adult minipigs; empty circles=juvenile minipigs.

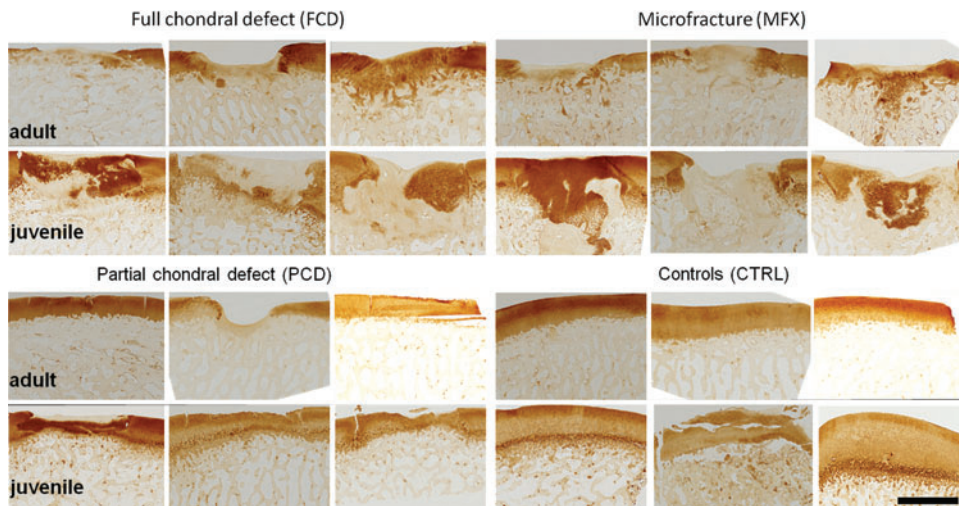


**FIG. 7.** Immunohistochemical staining for collagen type II; all samples are shown; juvenile minipigs showed more intense collagen II staining in FCD and MFX groups. Scale bar = 2 mm. Color images available online at [www.liebertpub.com/tec](http://www.liebertpub.com/tec)

in animal models,<sup>20</sup> this study investigated the extent of subchondral remodeling as a function of the type of cartilage lesion and skeletal maturity in a porcine model. We observed lesion- and age-dependent differences in subchondral bone remodeling at 6 weeks postoperatively, confirming our hypothesis. Interestingly, skeletally immature animals had more extensive subchondral bone remodeling compared with skeletally mature animals after the creation of full chondral defects (FCD) and full chondral defects that were treated by MFX. Subchondral bone remodeling after surgical creation of partial thickness chondral defects (PCD) resulted in elevated subchondral bone plates in skeletally immature animals. Age-related differences were also seen in cartilage repair, where more defect fill and qualitative improvement in the quality of repair tissue was observed in skeletally immature animals.

The initial subchondral bone loss in untreated and MFX-treated full thickness chondral defects (FCD) is most likely a consequence of multiple factors, including osteoclast activation, altered loading at the subchondral level, and the impact of synovial fluid permeating into the subchondral bone. Osteoclast activation after cartilage injury can partially be inhibited by bisphosphonates (e.g., risendronate<sup>20,21</sup>). Studies in rabbits and minipigs have also found a positive correlation between morphological restoration of the subchondral bone and cartilage repair capacity. It is well known that the health of subchondral bone is dependent on physiological load bearing.<sup>22</sup> In our study, animals were allowed full weightbearing immediately postoperatively, comparable to other previous studies that were restricted to skeletally immature animals.<sup>23–25</sup> In those studies, substantial subchondral remodeling was noted in the context of full chondral defects (FCD). Fisher *et al.*<sup>10</sup> developed a simple finite element model of load transmission in these full chondral defects, and they suggested that unloading of the underlying bone (due to the lack of load transmission by the missing cartilage in the defect) may contribute to subchondral remodeling.<sup>9,10,26</sup> Full chondral (FCD) and MFX groups showed substantial loss in bone beneath the defect, whereas PCD groups showed some evidence of overgrowth at 6 weeks postoperatively. These findings are consistent with previous reports in the literature.<sup>27</sup> In these partial chondral defects, the integrity of the osteochondral

junction was not disturbed and synovial fluid did not gain direct access to the subchondral bone.

The influence of age and skeletal maturity on subchondral bone remodeling after acute cartilage injury is not as well described. In studies of osteoarthritis, age is a factor in terms of bone quantity and quality, with specific changes occurring in subchondral architecture, biomechanical properties, and the balance between anabolic (by osteoblasts) and catabolic (by osteoclasts) processes.<sup>28,29</sup> In terms of acute injury, Murray *et al.*<sup>30</sup> described thickening of the subchondral bone plate and the calcified cartilage layer with age in an equine study, whereas Wei *et al.* found decreased volume fractions in the subchondral bone of young rabbits compared with adolescents and adults.<sup>28</sup> A thicker calcified cartilage layer as well as a thicker subchondral bone plate may protect the underlying bone from disturbance, and, therefore, result in less remodeling of the subchondral bone plate in skeletally mature animals. This is supported by our current findings, where more extensive subchondral remodeling was seen in juvenile (skeletally immature) animals.

A number of other experimental factors can influence the bone remodeling observed, including the choice of small versus large animal models and full thickness chondral versus osteochondral defects.<sup>19</sup> Other authors suggest that the initial degree of subchondral bone remodeling (within the first postoperative weeks) may be predictive of the long-term development of the subchondral bone and the osteochondral unit.<sup>20</sup> However, the exact temporal pattern of subchondral restoration appears to be species specific. Study timelines reach up to 1 year in rabbits,<sup>21,27,28,31</sup> sheep,<sup>13</sup> goats,<sup>32,33</sup> and horses.<sup>34</sup> Studies utilizing immature minipigs have noted subchondral remodeling, whether through gross or histological evaluation, at 6 months<sup>35</sup> and 1 year<sup>23</sup> follow-up. Although no animal model mimics the human situation completely,<sup>36</sup> all hallmarks that are observed in large animal models are also found in clinical studies of cartilage repair. For example, osseous overgrowth and cyst formation have been found repeatedly after cartilage repair in humans.<sup>5,7</sup> Moreover, it has been suggested that disturbance of the subchondral bone plate can be a main contributor to the failure of revision surgery in cartilage repair.<sup>3</sup>

In addition to changes in bone remodeling, our data also suggest poorer quality of repair cartilage in adult minipigs compared with juveniles. The size of cartilage defect required to establish a “critical” nonhealing state has been established in minipigs<sup>10</sup> as well as in goats<sup>37</sup> and dogs.<sup>38</sup> We found that defects of both ages filled to some extent with fibrous tissue, with defects in juvenile animals filling to a greater extent and being more likely to contain proteoglycans and type II collagen, indicative of better quality repair despite their more extensive subchondral remodeling. Whether these immature minipigs are able to compensate for the tremendous subchondral remodeling by producing more cartilage-like repair tissue remains to be investigated in further studies. Regardless of the cause, the bony remodeling needs to be addressed and/or accounted for in future studies of cartilage repair. As an example, it will be difficult to interpret findings from even the best tissue-engineered cartilage if it is placed atop a subchondral bone plate undergoing marked remodeling. A remodeling subchondral bone plate may likewise increase the risk of treatment failure for cell-based cartilage repair<sup>3</sup> and so speed the onset of osteoarthritis<sup>39</sup> as a consequence of altered biomechanical signals in the cartilaginous repair tissue.<sup>40</sup>

Additional time points are required to elucidate the full spatiotemporal pattern and extent of bony remodeling and defect fill in animal models and in humans as function of age. Further studies are also required to understand the causative mechanism of the subchondral bone remodeling in juveniles and the apparent decrease in cartilage formation in adults. Based on these findings, it is recommended that both preclinical and clinical studies of cartilage repair carefully evaluate and monitor changes in subchondral bone, for instance by using novel MRI imaging methods,<sup>41</sup> to avoid radiation exposure in patients.

## Conclusions

We compared subchondral bone remodeling after cartilage injury between skeletally mature and immature Yucatan minipigs. Our results suggest that subchondral bone remodeling is more extensive in skeletally immature animals at 6 weeks postoperatively in untreated and MFX-treated cartilage defects, whereas partial chondral defects showed upward migration of the subchondral bone plate in juveniles. The cartilage repair was of better quality in immature (juvenile) animals than in mature (adult) minipigs. These results can guide ongoing basic science and clinical studies investigating cartilage injuries and tissue engineering strategies.

## Acknowledgments

The authors would like to acknowledge assistance from Debra Pawlowski and Jeffrey House of the Philadelphia VA Medical Center Animal Research Facility, Niobra Keah for assistance with histological assays. This work was funded by the Department of Veterans Affairs (I01 RX000700), the AO Foundation, the National Institutes of Health, through the Penn Center for Musculoskeletal Disorders (P30 AR069619), and the German Research Foundation (DFG-PF 804/1-1).

## Authors' Contributions

C.G.P.: Study design, data collection, data analysis, interpretation of results, and article preparation; M.B.F.: Study

design, interpretation of results, and preparation of the article; V.S.: Data collection, interpretation of results; M.K.: Data collection; E.A.H.: Data collection, data analysis; D.A.S.: Funding, study design, and interpretation of results; G.R.D.: Funding, study design, data collection, and interpretation of results; R.L.M.: Funding, study design, interpretation of results, and article preparation. All authors have read and approved this article.

## Disclosure Statement

No competing financial interests exist.

## References

1. Mithoefer, K., Venugopal, V., and Manaqibwala, M. Incidence, degree, and clinical effect of subchondral bone overgrowth after microfracture in the knee. *Am J Sports Med* **44**, 2057, 2016.
2. Saris, D.B., Vanlauwe, J., Victor, J., *et al.* Treatment of symptomatic cartilage defects of the knee: characterized chondrocyte implantation results in better clinical outcome at 36 months in a randomized trial compared to microfracture. *Am J Sports Med* **37 Suppl 1**, 10s, 2009.
3. Minas, T., Gomoll, A.H., Rosenberger, R., *et al.* Increased failure rate of autologous chondrocyte implantation after previous treatment with marrow stimulation techniques. *Am J Sports Med* **37**, 902, 2009.
4. Henderson, I.J., and La Valette, DP. Subchondral bone overgrowth in the presence of full-thickness cartilage defects in the knee. *Knee* **12**, 435, 2005.
5. Cole, B.J., Farr, J., Winalski, C.S., *et al.* Outcomes after a single-stage procedure for cell-based cartilage repair: a prospective clinical safety trial with 2-year follow-up. *Am J Sports Med* **39**, 1170, 2011.
6. Kreuz, P.C., Steinwachs, M.R., Erggelet, C., *et al.* Results after microfracture of full-thickness chondral defects in different compartments in the knee. *Osteoarthritis Cartilage* **14**, 1119, 2006.
7. Vasiliadis, H.S., Danielson, B., Ljungberg, M., *et al.* Autologous chondrocyte implantation in cartilage lesions of the knee: long-term evaluation with magnetic resonance imaging and delayed gadolinium-enhanced magnetic resonance imaging technique. *Am J Sports Med* **38**, 943, 2010.
8. Breinan, H.A., Minas, T., Hsu, H.P., *et al.* Effect of cultured autologous chondrocytes on repair of chondral defects in a canine model. *J Bone Joint Surg Am* **79**, 1439, 1997.
9. Vasara, A.I., Hyttinen, M.M., Lammi, M.J., *et al.* Subchondral bone reaction associated with chondral defect and attempted cartilage repair in goats. *Calcif Tissue Int* **74**, 107, 2004.
10. Fisher, M.B., Belkin, N.S., Milby, A.H., *et al.* Cartilage repair and subchondral bone remodeling in response to focal lesions in a mini-pig model: implications for tissue engineering. *Tissue Eng Part A* **21**, 850, 2015.
11. Chen, H., Chevrier, A., Hoemann, C.D., *et al.* Characterization of subchondral bone repair for marrow-stimulated chondral defects and its relationship to articular cartilage resurfacing. *Am J Sports Med* **39**, 1731, 2011.
12. Shamis, L.D., Bramlage, L.R., Gabel, A.A., and Weisbrode, S. Effect of subchondral drilling on repair of partial-thickness cartilage defects of third carpal bones in horses. *Am J Vet Res* **50**, 290, 1989.
13. Dorotka, R., Bindreiter, U., Macfelda, K., *et al.* Marrow stimulation and chondrocyte transplantation using a collagen



- matrix for cartilage repair. *Osteoarthritis Cartilage* **13**, 655, 2005.
14. Gomoll, A.H., Madry, H., Knutsen, G., *et al.* The subchondral bone in articular cartilage repair: current problems in the surgical management. *Knee Surg Sports Traumatol Arthrosc* **18**, 434, 2010.
  15. Rauch, F., Travers, R., and Glorieux, F.H. Intracortical remodeling during human bone development—a histomorphometric study. *Bone* **40**, 274, 2007.
  16. Busse, B., Djonic, D., Milovanovic, P., *et al.* Decrease in the osteocyte lacunar density accompanied by hypermineralized lacunar occlusion reveals failure and delay of remodeling in aged human bone. *Aging Cell* **9**, 1065, 2010.
  17. Goebel, L., Orth, P., Muller, A., *et al.* Experimental scoring systems for macroscopic articular cartilage repair correlate with the MOCART score assessed by a high-field MRI at 9.4 T—comparative evaluation of five macroscopic scoring systems in a large animal cartilage defect model. *Osteoarthritis Cartilage* **20**, 1046, 2012.
  18. Mainil-Varlet, P., Van Damme, B., Nesic, D., *et al.* A new histology scoring system for the assessment of the quality of human cartilage repair: ICRS II. *Am J Sports Med* **38**, 880, 2010.
  19. Orth, P., Cucchiari, M., Kohn, D., and Madry, H. Alterations of the subchondral bone in osteochondral repair—translational data and clinical evidence. *Eur Cell Mater* **25**, 299–316; discussion 314, 2013.
  20. Muehleman, C., Li, J., Abe, Y., *et al.* Effect of risedronate in a minipig cartilage defect model with allograft. *J Orthop Res* **27**, 360, 2009.
  21. Nishitani, K., Shirai, T., Kobayashi, M., *et al.* Positive effect of alendronate on subchondral bone healing and subsequent cartilage repair in a rabbit osteochondral defect model. *Am J Sports Med* **37 Suppl 1**, 139S, 2009.
  22. Yokota, H., Leong, D.J., and Sun, H.B. Mechanical loading: bone remodeling and cartilage maintenance. *Curr Osteoporos Rep* **9**, 237, 2011.
  23. Vasara, A.I., Hyttinen, M.M., Pulliainen, O., *et al.* Immature porcine knee cartilage lesions show good healing with or without autologous chondrocyte transplantation. *Osteoarthritis Cartilage* **14**, 1066, 2006.
  24. Kim, I.L., Pfeifer, C.G., Fisher, M.B., *et al.* Fibrous scaffolds with varied fiber chemistry and growth factor delivery promote repair in a porcine cartilage defect model. *Tissue Eng Part A* **21**, 2680, 2015.
  25. Fisher, M.B., Belkin, N.S., Milby, A.H., *et al.* Effects of mesenchymal stem cell and growth factor delivery on cartilage repair in a mini-pig model. *Cartilage* **7**, 174, 2016.
  26. Yokota, M., Yasuda, K., Kitamura, N., *et al.* Spontaneous hyaline cartilage regeneration can be induced in an osteochondral defect created in the femoral condyle using a novel double-network hydrogel. *BMC Musculoskelet Disord* **12**, 49, 2011.
  27. Orth, P., Cucchiari, M., Kaul, G., *et al.* Temporal and spatial migration pattern of the subchondral bone plate in a rabbit osteochondral defect model. *Osteoarthritis Cartilage* **20**, 1161, 2012.
  28. Wei, X., Gao, J., and Messner, K. Maturation-dependent repair of untreated osteochondral defects in the rabbit knee joint. *J Biomed Mater Res* **34**, 63, 1997.
  29. Zimmermann, E.A., Schaible, E., Bale, H., *et al.* Age-related changes in the plasticity and toughness of human cortical bone at multiple length scales. *Proc Natl Acad Sci U S A* **108**, 14416, 2011.
  30. Murray, R.C., Blunden, T.S., Branch, M.V., *et al.* Evaluation of age-related changes in the structure of the equine tarsometatarsal osteochondral unit. *Am J Vet Res* **70**, 30, 2009.
  31. Shapiro, F., Koide, S., and Glimcher, M.J. Cell origin and differentiation in the repair of full-thickness defects of articular cartilage. *J Bone Joint Surg Am* **75**, 532, 1993.
  32. Shahgaldi, B.F., Amis, A.A., Heatley, F.W., *et al.* Repair of cartilage lesions using biological implants. A comparative histological and biomechanical study in goats. *J Bone Joint Surg Br* **73**, 57, 1991.
  33. Jackson, D.W., Lalor, P.A., Aberman, H.M., and Simon, T.M. Spontaneous repair of full-thickness defects of articular cartilage in a goat model. A preliminary study. *J Bone Joint Surg Am* **83-A**, 53, 2001.
  34. Frisbie, D.D., Trotter, G.W., Powers, B.E., *et al.* Arthroscopic subchondral bone plate microfracture technique augments healing of large chondral defects in the radial carpal bone and medial femoral condyle of horses. *Vet Surg* **28**, 242, 1999.
  35. Li, W.J., Chiang, H., Kuo, T.F., *et al.* Evaluation of articular cartilage repair using biodegradable nanofibrous scaffolds in a swine model: a pilot study. *J Tissue Eng Regen Med* **3**, 1, 2009.
  36. Chevrier, A., Kouao, A.S., Picard, G., *et al.* Interspecies comparison of subchondral bone properties important for cartilage repair. *J Orthop Res* **33**, 63, 2015.
  37. Jeng, L., Hsu, H.P. and Spector, M. Tissue-engineered cartilaginous constructs for the treatment of caprine cartilage defects, including distribution of laminin and type IV collagen. *Tissue Eng Part A* **19**, 2267, 2013.
  38. Breinan, H.A., Minas, T., Hsu, H.P., *et al.* Autologous chondrocyte implantation in a canine model: change in composition of reparative tissue with time. *J Orthop Res* **19**, 482, 2001.
  39. Lajeunesse, D., Hilal, G., Pelletier, J.P., and Martel-Pelletier, J. Subchondral bone morphological and biochemical alterations in osteoarthritis. *Osteoarthritis Cartilage* **7**, 321, 1999.
  40. Qiu, Y.S., Shahgaldi, B.F., Revell, W.J., and Heatley, F.W. Observations of subchondral plate advancement during osteochondral repair: a histomorphometric and mechanical study in the rabbit femoral condyle. *Osteoarthritis Cartilage* **11**, 810, 2003.
  41. Eley, K.A., Watt-Smith, S.R., and Golding, S.J. “Black bone” MRI: a potential alternative to CT when imaging the head and neck: report of eight clinical cases and review of the Oxford experience. *Br J Radiol* **85**, 1457, 2012.

Address correspondence to:

Robert L. Mauck, PhD

Department of Orthopaedic Surgery

Perelman School of Medicine

University of Pennsylvania

424 Stemmler Hall, 36th Street and Hamilton Walk

Philadelphia, PA 19104

E-mail: lemauck@mail.med.upenn.edu

Received: March 7, 2017

Accepted: July 11, 2017

Online Publication Date: October 26, 2017